

Figure S1: Results of the differential abundance analysis on antibiotic class level for mom samples. **A-C)** Changes in abundance of class level antibiotic resistance in moms at different timepoints, as determined by using DESeq2. Log2 fold changes of antibiotic classes are shown on the x-axis, where a log2 fold change of 0 is marked by the dashed line. Classes are coloured based on significance, where blue indicates a significant (adjusted p-value < 0.05) change in abundance, and grey indicates that there was no difference in abundance between groups. The group that is mentioned second in the name of the comparison was set as the reference group. Timepoints are abbreviated, where B= baseline, M= midline, and E= endline. **D)** BaseMean, as calculated by DESeq2, which indicates the mean abundance of the antibiotic classes in all human samples.

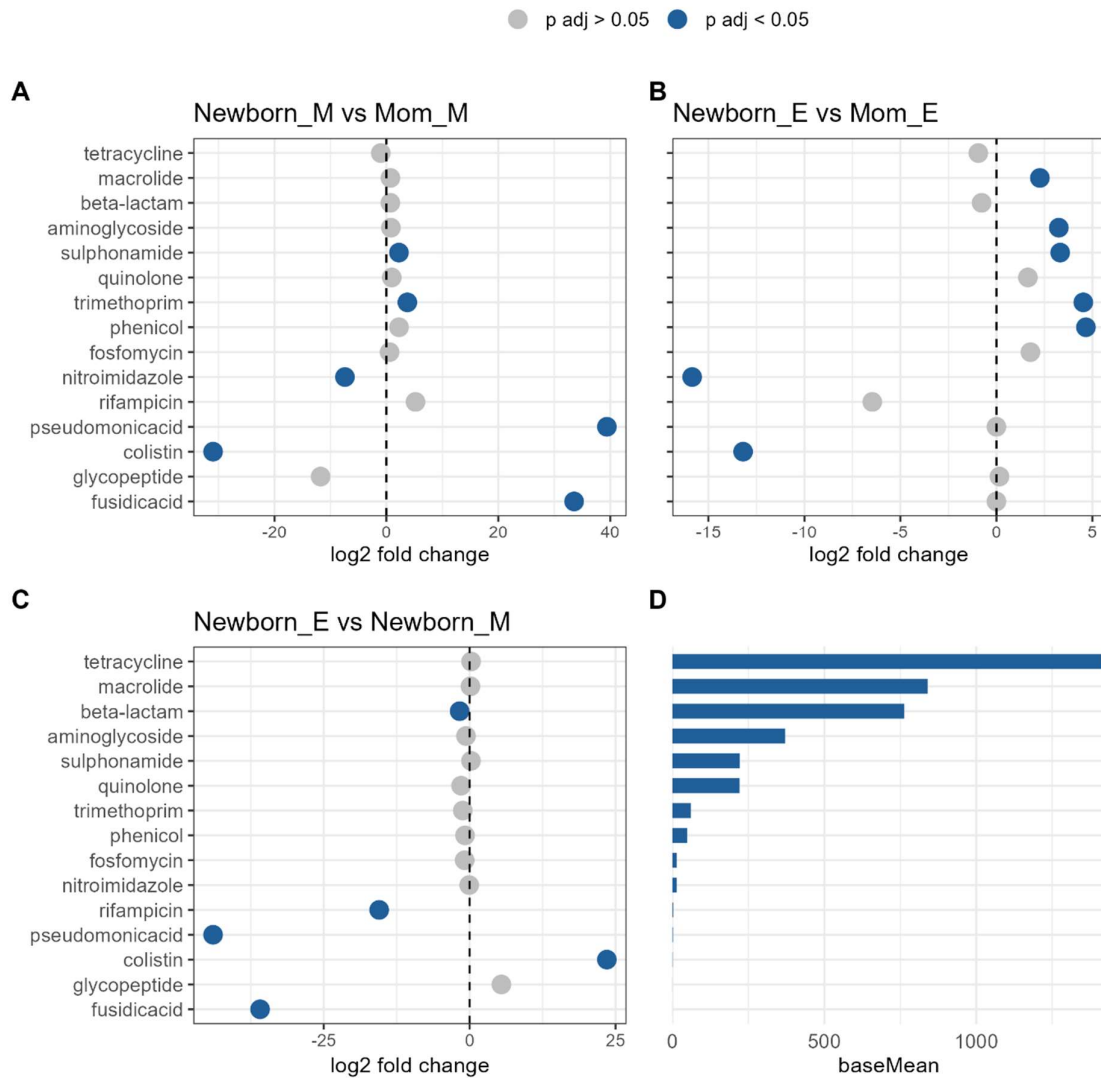


Figure S2: Results of the differential abundance analysis on antibiotic class level for newborn and mom samples. **A-C)** Changes in abundance of class level antibiotic resistance in newborns at different timepoints and differences with the antibiotic class resistance in mom samples, as determined by using DESeq2. Log₂ fold changes of antibiotic classes are shown on the x-axis, where a log₂ fold change of 0 is marked by the dashed line. Classes are coloured based on significance, where blue indicates a significant (adjusted p-value < 0.05) change in abundance, and grey indicates that there was no difference in abundance between groups. The group that is mentioned second in the name of the comparison was set as the reference group. Timepoints are abbreviated, where B= baseline, M= midline, and E= endline. **D)** BaseMean, as calculated by DESeq2, which indicates the mean abundance of the antibiotic classes in all human samples.

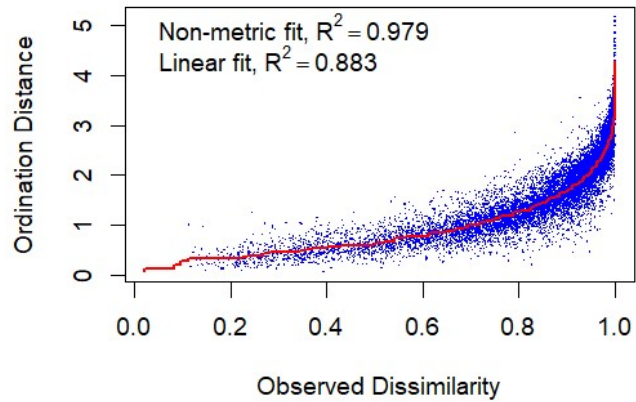


Figure S3: Shepard diagram of the NMDS ordination that was made on Bray-Curtis distances between ARG counts of all samples in the dataset ($k=3$, stress value=0.14). Plot was made with the stressplot function implemented in the vegan package in R.

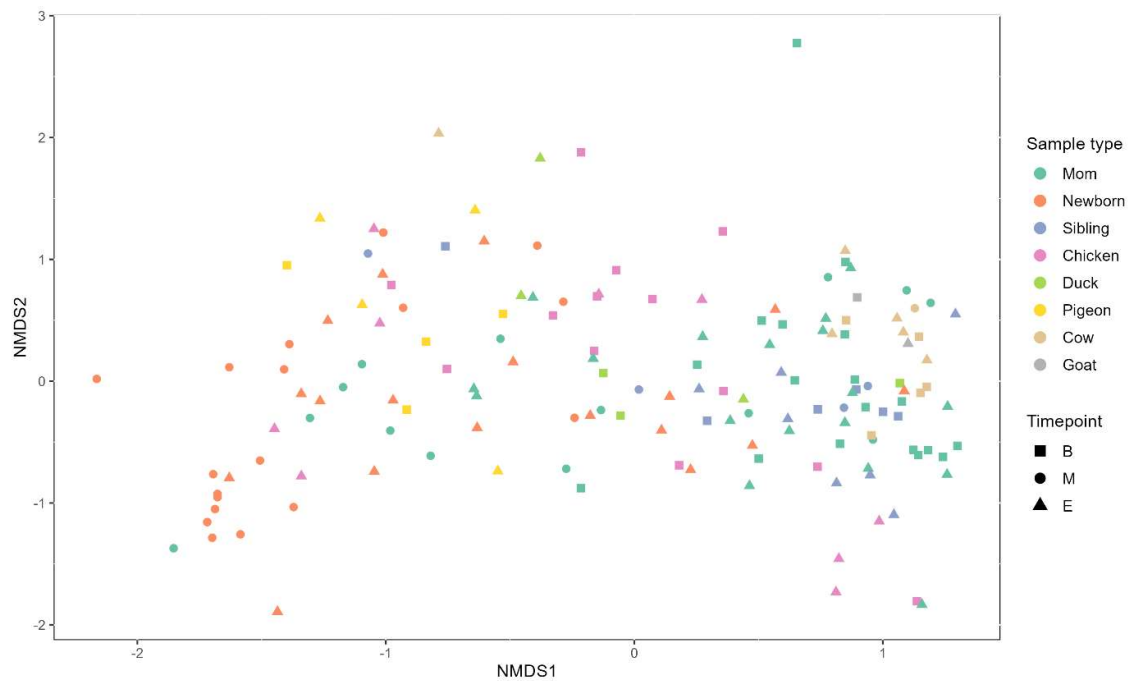


Figure S4: First two axis of the NMDS ordination on Bray-Curtis dissimilarities between ARG counts (FPKM) in all samples. Each point represents one sample, where sample type is indicated by the colour of the points, and the timepoint is indicated by the shape. Timepoints are abbreviated, where B= baseline, M= midline, and E= endline.

Table S1: Results of the PERMANOVA that was carried out on the Bray-Curtis dissimilarities between ARG counts (FPKM) in all samples. *** p-value < 0.001, ** p-value < 0.01, * p-value < 0.05.

Factor	R2	p-value
Sample type	0.18	0.001 ***
Timepoint	0.04	0.001 ***
Household	0.11	0.035 *
Sample type : timepoint	0.05	0.360
Household : sample type	0.30	0.027 *
Household : timepoint	0.18	0.217

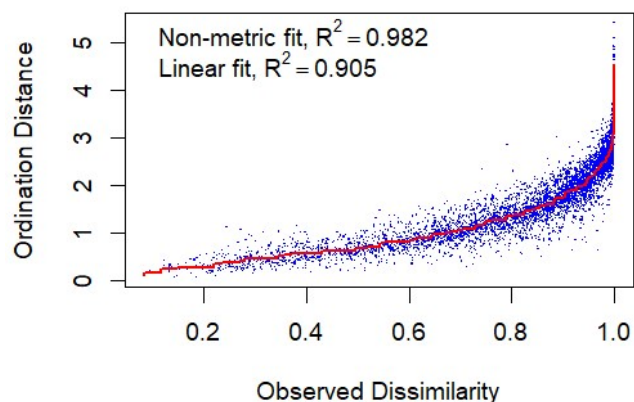


Figure S5: Shepard diagram of the NMDS ordination that was made on Bray-Curtis distances between ARG counts of all human samples in the dataset ($k = 3$, stress value = 0.13). Plot was made with the stressplot function implemented in the vegan package in R.

Table S2: Dynamics of the ARGs that were significantly more abundant in moms at midline compared to moms at baseline, as determined by DESeq2 analysis. Per gene, the DESeq2 normalized gene count at baseline (B), midline (M), and endline (E) is listed. Gene group indicates if ARGs remain more abundant at endline or recover to similar levels as the midline samples. If the gene group is “unclear”, this indicates that there were no significant differences for the endline vs baseline comparison and neither for the endline vs midline comparison, meaning that it could not be said if the ARG remained as abundant at endline as it was at midline, or if it decreased to be similar to baseline.

Gene name	B	M	E	Gene group
ant(3'')-la_1	1,509842	25,95452	5,128981	unclear
mph(A)_2	27,11701	49,20903	1,821109	goesdown
ant(6)-la_5	0,160856	11,1048	0,206007	goesdown
blaSHV-2a_1	1,043109	32,36748	3,342813	remainshigh
blaCTX-M-1_1	0,010432	281,8602	0,247144	goesdown
mph(E)_1	0,022155	10,16107	0	goesdown
sul1_2	57,95311	126,995	59,84039	goesdown
blaCTX-M-64_1	0,002014	1,440773	0,003633	goesdown
ant(6)-la_2	0,008554	14,29032	0,040812	goesdown
aac(3)-la_1	0,00481	179,8946	0,30655	goesdown
blaTEM-1A_1	0,963544	175,4467	13,22377	goesdown
erm(X)_1	4,488506	74,2749	7,200192	goesdown

aph(6)-ld_1	1,391751	128,3716	38,15761	remainshigh
aadA11_2	0,843331	15,25087	1,128218	goesdown
aph(3'')-lb_1	1,020621	102,1161	36,62293	unclear
erm(T)_1	0,859546	36,23431	0,434537	unclear
qnrS1_1	0,338578	37,22005	12,53216	remainshigh
OqxB_1	8,025281	190,3479	34,36569	remainshigh
aac(6')-li_1	0	20,11579	0	goesdown
tetB(46)_1	0,892175	16,08885	0,269974	goesdown
dfrA12_1	0,061826	9,008956	0,197841	goesdown
tetA(46)_1	1,117896	19,45702	0,344336	goesdown
fosA5_1	0,82163	20,38921	3,122958	remainshigh
msr(C)_1	0,007237	57,28648	0	goesdown
aph(2'')-la_2	0,223727	20,481	0,105078	goesdown
msr(E)_1	0,037449	21,66169	0,078159	goesdown
msr(D)_2	4,216594	42,74879	7,351441	goesdown
aac(6')-lb_2	0	124,6022	0,005312	goesdown
tet(L)_2	1,823735	79,21969	2,374442	goesdown
mef(A)_4	3,551794	36,91916	5,615266	goesdown
tet(B)_1	0,129753	17,92331	14,68095	unclear
OqxA_1	2,808494	62,35991	8,855676	remainshigh

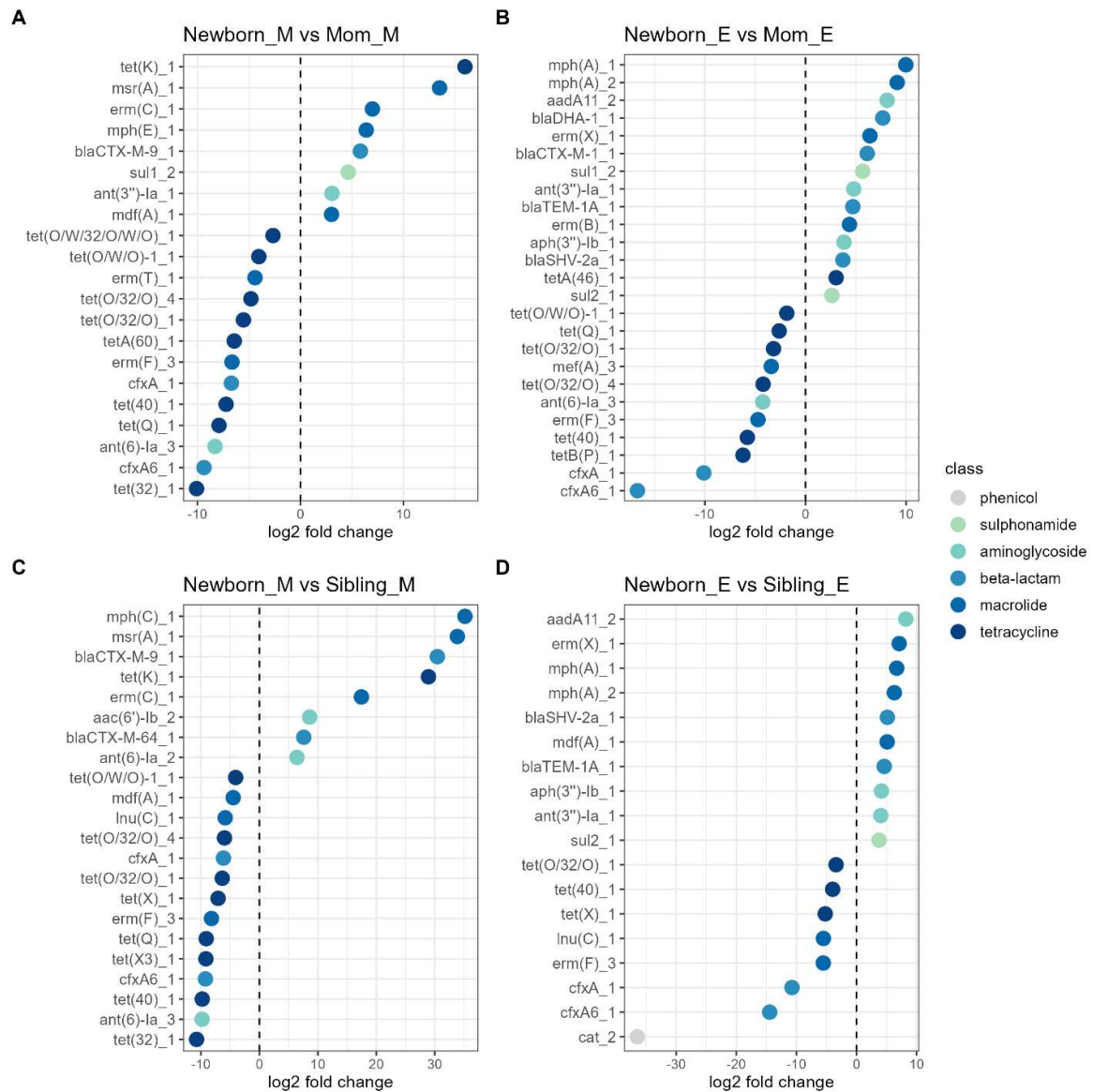


Figure S6: Significantly (*adjusted p-value* < 0.05) differently abundant ARGs in comparisons between newborns and moms or newborns and siblings at midline and endline, as determined by using DESeq2. Log₂ fold changes of ARGs are shown on the x-axis, where a log₂ fold change of 0 is marked by the dashed line. Genes are coloured based on the class of antibiotics that they confer resistance to. In **A-D**, the group that is mentioned second in the name of the comparison was set as the reference group. Timepoints are abbreviated, where B= baseline, M= midline, and E= endline.

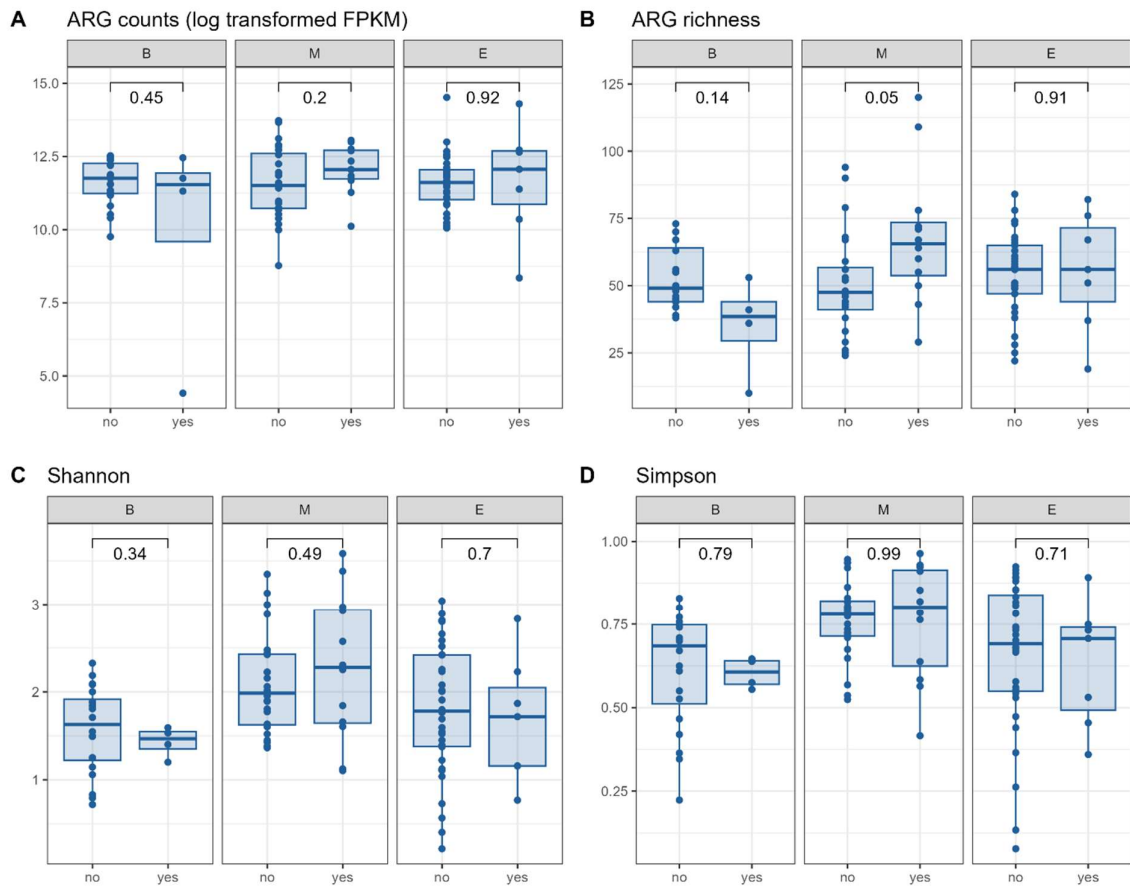


Figure S7: ARG abundance and alpha diversity of people for whom no or any antibiotic use was registered for the timepoint at which the sample was taken. **A)** ARG counts (log transformed FPKM values), **B)** ARG richness, **C)** Shannon diversity, and **D)** Simpson diversity, at different timepoints. Timepoints are abbreviated, where B= baseline, M= midline, and E= endline. Depicted p-values were obtained by performing two-sided t-tests on the value of the different measures and the within timepoint antibiotic use (value ~ AB usage), which was done separately for each timepoint.

Table S3: Differently abundant ARGs (adjusted p-value < 0.05) that resulted from the DESeq2 analysis which compared moms at midline who did not use antibiotics versus those who used antibiotics of any kind. Moms at midline who did not use antibiotics were set as the reference group, meaning that ARGs with a positive log2 fold change were more abundant in moms at midline who used antibiotics compared to those who had not used antibiotics.

Gene name	Antibiotic class	log2FoldChange	padj
tetA(46)_1	tetracycline	5.449427	0.040023
mph(A)_2	macrolide	8.247145	0.0028
mph(A)_1	macrolide	9.849035	0.000376
blaNDM-19_1	beta-lactam	9.660721	0.004479
aadA11_2	aminoglycoside	9.668913	0.000513
erm(F)_3	macrolide	7.986061	0.000513
dfrA12_1	trimethoprim	6.95673	0.040023

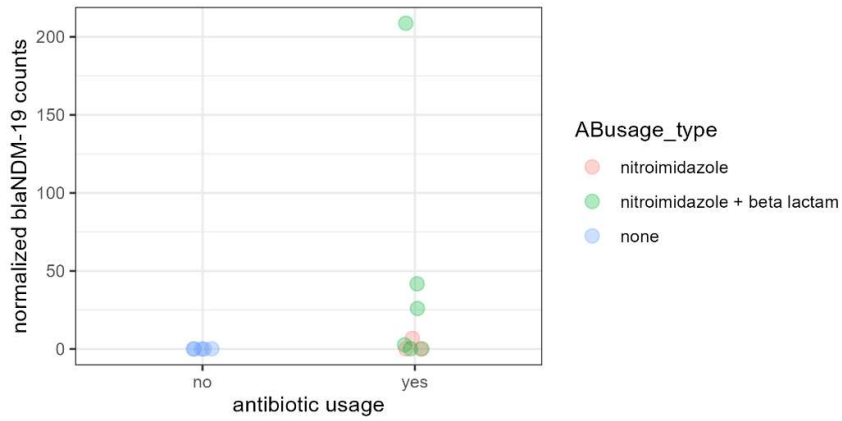


Figure S8: DESeq2 normalized counts of blaNDM-19 in mom samples at midline. Groups were based on within timepoint antibiotic usage, where it was noted if moms had used any antibiotics within a week prior to sampling (yes/no). Colour of points indicates which antibiotic was used. Jitter was added to show overlapping points.

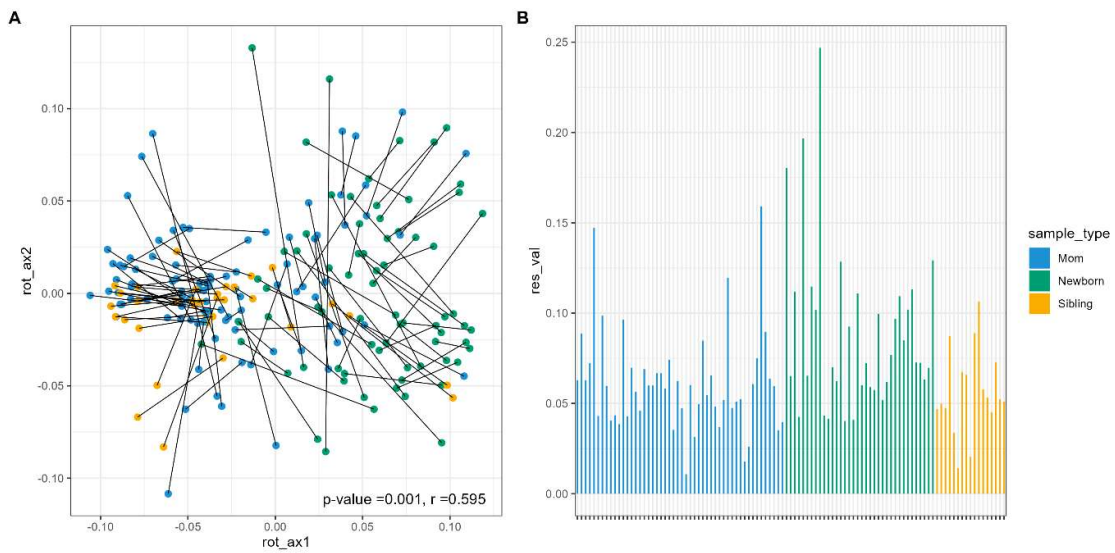


Figure S9: Rotation (A) and residuals (B) plots from the Procrustes analysis with NMDS ordinations on Bray-Curtis distances from the resistome and the microbiome counts for human samples at all timepoints. Colours indicate different sample types.

were filtered on significance (BH adjusted p -value < 0.01) and robustness ($\rho > 0.8$). In **B**) correlations were filtered on significance (BH adjusted p -value < 0.01) and robustness ($\rho > 0.7$). Additionally, correlations that included tet(40) or tet(O/32/O) were significant in this network, but were filtered out.

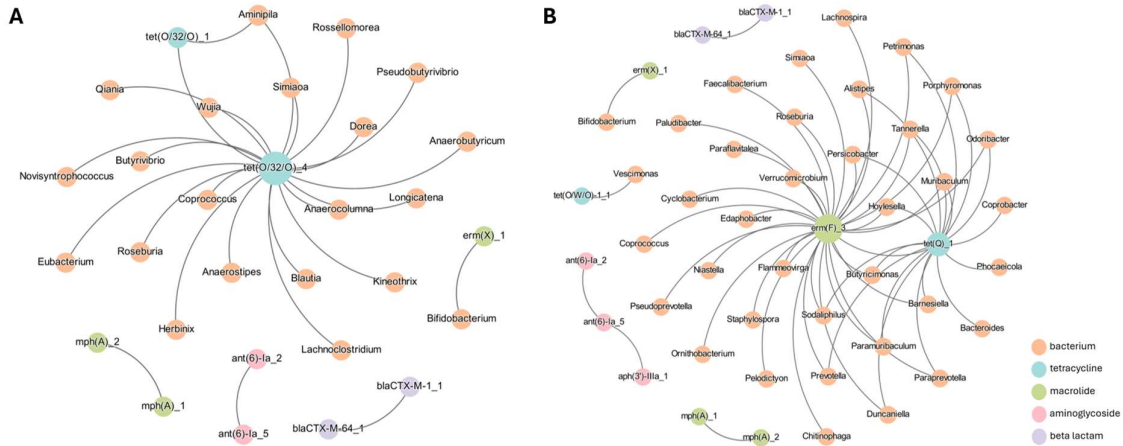


Figure S12: Fruchterman-Reingold representation of the co-occurrences between all microbial taxa and the differentially abundant ARGs in newborns at endline compared to midline. ARG-ARG and ARG-bacteria co-occurrences were determined by calculating Spearman's correlations between ARG and bacterial counts. Node size represents the degree of connectedness, and node colour represents the different antimicrobial classes or a bacterial genus. In **A**) correlations were filtered on significance (BH adjusted p -value < 0.01) and robustness ($\rho > 0.8$). In **B**) correlations were filtered on significance (BH adjusted p -value < 0.01) and robustness ($\rho > 0.7$). Additionally, correlations that included tet(40) or tet(O/32/O) were significant in this network, but were filtered out.

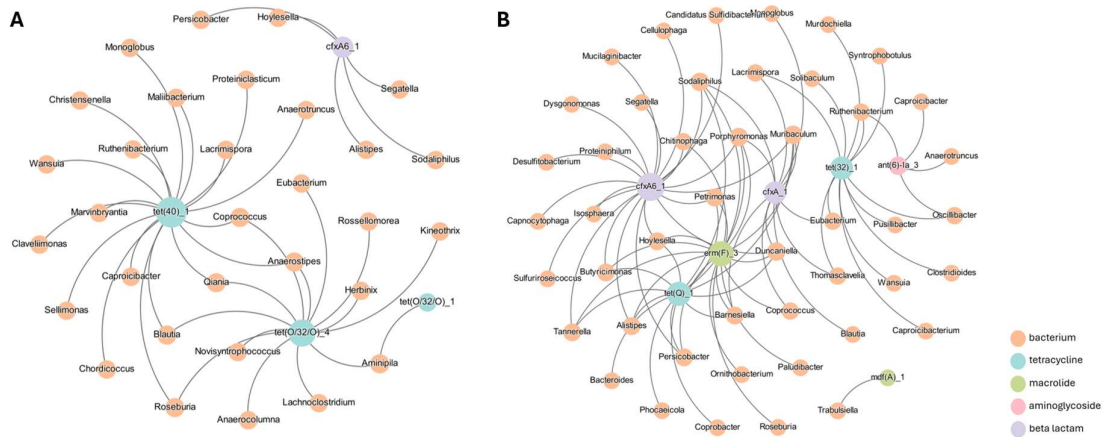


Figure S13: Fruchterman-Reingold representation of the co-occurrences between all ARGs and the differentially abundant microbial genera in newborns at endline compared to midline. ARG-ARG and ARG-bacteria co-occurrences were determined by calculating Spearman's correlations between ARG and bacterial counts. Node size represents the degree of connectedness, and node colour represents the different antimicrobial classes or a bacterial genus. In **A**) correlations were filtered on significance (BH adjusted p -value < 0.01) and robustness ($\rho > 0.8$). In **B**) correlations were filtered on significance (BH adjusted p -value < 0.01) and robustness ($\rho > 0.7$). Additionally, correlations that included tet(40) or tet(O/32/O) were significant in this network, but were filtered out.